Development of Scintillating Fiber Imager

Kouji Morimoto[1], Fuyuki Tokanai[1,2], Isao Tanihata[1], Yoshihide Hayashizaki[1]
[1]The Institute of Physical and Chemical Research (RIKEN), Japan
[2]Japan Science and Technology Corporation (JST), Japan

Abstract

A Scintillating Fiber Imager (SFI) has been developed for Restriction Landmark Genomic Scanning (RLGS) technology. Test measurements have been carried out with genomic linkage map labeled with ^{32}P (β-ray emitter) and ^{58}Ni beam at 90 A MeV as well. The system offers real time acquisition and an easy quantification of RLGS data compared to film-based autoradiography, and it is proved to be a powerful position sensitive detector for measurements in nuclear physics.

I. Introduction

The Restriction Landmark Genomic Scanning (RLGS) technology is a powerful and relatively rapid method for the genetic analysis of mouse and human genome as well as that of other animals and plants (e.g. [1, 2]). RLGS employs direct end labeling of the genomic DNA digested with a restriction enzyme, high resolution two-dimensional gel electrophoresis, and *autoradiography*. The restriction enzyme site labeled with beta-emitting radionuclide of ^{32}P can be used as landmark loci. Hereafter we call the restriction enzyme genome spot. There are more than two thousand genome spots in a single dried gel of 40 x 40 cm^2. Film-based autoradiography is one of the most useful methods to obtain the genomic information, because of its large detection area and excellent position resolution. However, it has two disadvantages i.e., 1) long exposure time (about two weeks) due to the low sensitivity, and 2) lack of quantitative information due to the non-linearity of response and limited dynamic range. These disadvantages can be overcome by using scintillation fibers. The purpose of this work is to develop a Scintillating Fiber Imager (SFI) for the RLGS technology with faster analyzing time than the film-based autoradiography and with quantitative information.

Recently, successful applications of scintillating fibers have been reported not only for high-energy physics as tracking detectors [3, 4], but also for molecular biology in DNA sequencing [5, 6]. The main advantages of scintillating fibers are the flexibility of the fibers and the thin diameter (250μm can be reached) providing excellent position resolution. It can also provide very large detection area with good position resolution for the RLGS technology. SFI for RLGS is based on the detection of β-ray source (minimum ionization particle) of ^{32}P where the maximum energy is 1.7 MeV. Multi-Anode PhotoMultiplier Tubes (MAPMTs) are applied as SFI read-out device. Therefore, it is very important that MAPMT has gain uniformity and stability, pixel uniformity, linearity, well known cross talk and quantum efficiency, since it is expected that only few photons reach the end of the fibers. For these reasons, we investigated the performance of SFI for relativistic heavy ions, because the energy loss of heavy ions is larger than that of minimum ionization particle at the same incident energy.

In section 2 we describe the SFI system including the fiber, MAPMT, and the data acquisition system. Section 3 describes the result of SFI for RLGS and performance of SFI. Section 4 describes the further plans to improve the performance of SFI.

II. Description of the Detector

The basic principle of Scintillating Fiber Imager (SFI) is shown in Figure 1. Two orthogonal fiber-layers are placed on the dried gel sheet containing the genome spots labeled with β-ray source of ^{32}P. The β-ray penetrates both fiber planes and produces a visible photon emission. These photons are transmitted to both ends of fiber. The Multi-Anode PhotoMultipliers Tube (MAPMT) detects it and sends the signal to electronics. The signal is analyzed by the encoding method as follows.

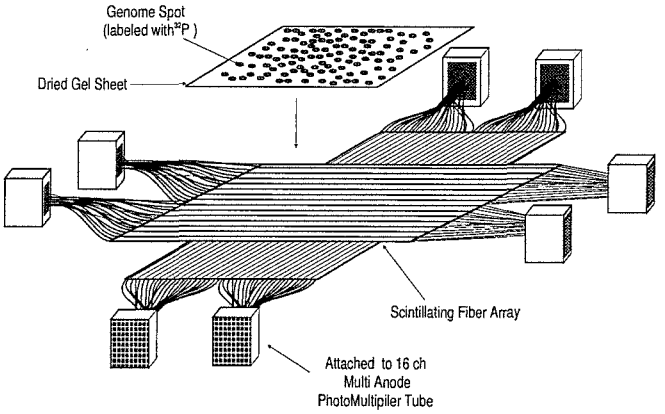

Figure 1: Basic principle of Scintillating Fiber Imager (SFI)

The SFI includes four identical sets of scintillation fiber layers, each layer consists of 256 fibers. The fibers have a square cross-section of 0.8 mm^2(BICRON BCF-12 type) [7]. Two of them give X-directional position and the others give Y-directional position. This effective area 43 x 43 cm^2 can easily cover the area of a gel sheet (35 x 43 cm^2). The successful application of SFI in autoradiography depends on the ability to detect the few photons that reach the end of the fiber. Thus, we selected the multi-clad type fiber to increase the number of photons. Since the diameter of a typical genome spot is in the range of 3 – 5 mm

and the distance between neighboring spots is $\sim$ 5 mm, the required position resolution is about 1 mm for the autoradiography,

MAPMT of Hamamatsu R5900-L16[8] was used for SFI. This unit has 16 channels arranged in a linear array and an effective area of 16 $\times$ 16 mm^2. The 16 channel anodes are arranged with 0.8 mm pitch and 0.2 mm dead spaces, the gain uniformity between each anode is about 80%, as reported by the manufacturer [9]. The typical gain is about 2 $\times$ 10^6 at the operating voltage of -800 V. The specification of the cross-talk between each anode is typically about 3%, small enough to reject cross-talk events even at large number of photons produced in the fiber.

Since the SFI has many fibers, we used a matrix method as shown in Figure 2. Thus, we can avoid using too many MAPMT's and electronics. Each side of 256 fibers was arranged into a 16 $\times$ 16 matrix. One end of the fiber matrix is attached to a MAPMT to read lateral 16 lines information and the other side is to read vertical 16 line information. One of the MAPMT gives the information package of 16 fibers (belt) and the other gives individual information of each package of 16 fibers (strip). Therefore, 256 fibers can be decoded by the two set of 16 channel MAPMT, hence we succeeded in reducing the number of readout channels of the 1024 fibers to 128 channels.

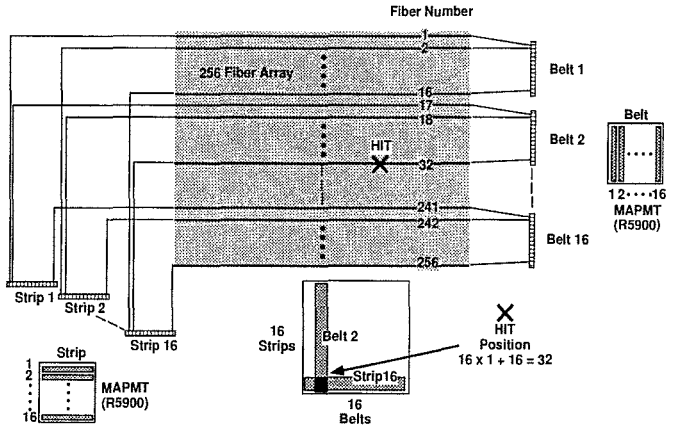

Figure 2: Repetition of the 256 scintillating fiber unit on the MAPMTs. In this method the unit of 256 fibers can be read out with 32 channels.

The signals from MAPMT are amplified by pre-amplifiers and sent to discriminator with variable threshold level for each channel. Because the MAPMT's gain is different for each channel, the threshold level should be changed according to each channel. In addition, the MAPMT noise can be reduced by triggering to coincidence events between both sides of fibers and both layers. The hit patterns of the discriminator are sent to computer via the CAMAC system. The decoding of the hit pattern from discriminator and data acquisition can be done simultaneously on the computer, allowing the observation of the images in real time.

III. Performance of the SFI

The spatial resolutions of SFI were measured using 1 MeV and 0.5 MeV internal-conversion electrons from a ^{207}Bi source with a diameter of 3 mm. The position histograms for the X-axis and Y-axis are shown in Figure 3a and 3b, respectively. These spatial resolutions for the 3 mm diameter beta-ray source is 4.8 mm (FWHM) for X-axis and 5.6 mm (FWHM) for Y-axis, respectively. The relatively poor resolution of Y-axis is due to the long range of β-ray in the detector. Since the difference is much smaller than the distance between neighboring genome spots and the diameter of a typical genome spot, it does not influence the identification of genome spot for RLGS.

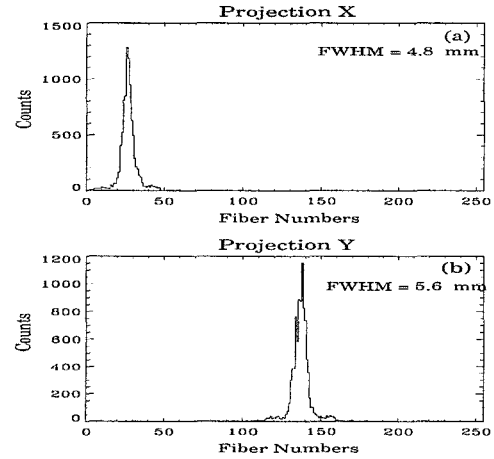

Figure 3: Position histograms of X axis (a) and Y axis (b) for the 3 mm diameter ^{207}Bi source.

Figure 4 shows the β-ray pulse height distribution of a ^{90}Sr source with end-point energy of 2.27 MeV. This is close to that of 1.71 MeV for ^{32}P. The single and double photo-electron peaks are clearly seen. Since the quantum efficiency of this MAPMT is about 15%, the average number of photons reached the end of fiber is around 10 per event.

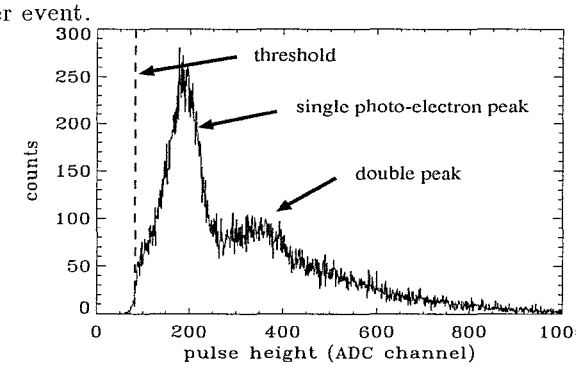

Figure 4: Pulse height spectrum of β-ray from ^{90}Sr source. The single and double photo-electron peaks are clearly seen. The single photo-electron peak contains the signal from the β-ray and the thermal noise of the MAPMT.

The threshold for each anode was set to a value below the single photo-electron peak to get the RLGS images with high detection efficiency. Although the photo-electron peak contains the thermal noise of the MAPMT, the random coincidence of the eight MAPMTs is extremely small. Therefore, the thermal noise events can be almost entirely rejected by triggering the events to the coincidence between both sides of fibers and both layers.

A. *Detection of RLGS map*

The Restriction Landmark Genomic Scanning (RLGS) map used in the detector test was processed at the Genomic Science Laboratory of RIKEN. The map was electrophoresised to two dimensional and dried on filter paper. There are more than one thousand genome spots in a single dried gel sheet of 20 x 20 cm^2. We carried out the observation of the genome spots labeled with ^{32}P one day after the RLGS process.

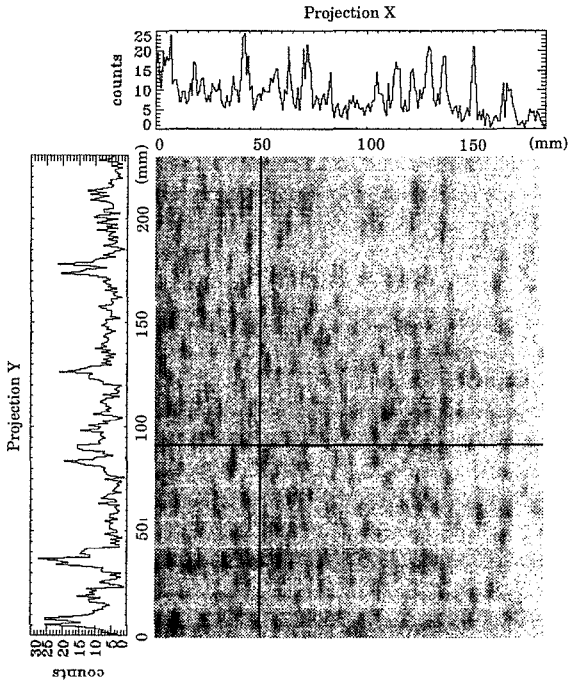

Figure 5: Image of RLGS map labeled with ^{32}P. The genome spots are clearly seen.

Figure 5 shows the image of genome spots in a single dried gel sheet. The genomic spots are clearly seen and each one can be distinguished. It took about 50 hours to accumulate statistics applicable to quantitative analysis. This shows that SFI needs much shorter time to measure the RLGS map compared to the film-based autoradiography, since the autoradiography takes about two weeks to get the image. However, the detection efficiency was smaller than that of we expected (roughly 12 hours). This lack of detection efficiency could be explained by the cross-talk of scintillating photons at joining points between the fibers and the photo-cathode of MAPMT, since the anode pitch of this MAPMT is too narrow to collect all of the photons emitted by corresponding fibers. Therefore, it is very important to investigate the cross-talk ratio not only with β-ray source (minimum ionization particle), but about with relativistic heavy ions.

IV. Calibration of SFI with ^{58}Ni beam

In order to investigate the cross talk between fibers and the photo-cathode of MAPMT, we carried out test measurement with heavy ions produced by the RIKEN Ring Cyclotron. The incident beam was ^{58}Ni at 90 AMeV energy and the beam rate were up to 10^5 particles/sec. The layout of the detectors is illustrated in Figure 6.

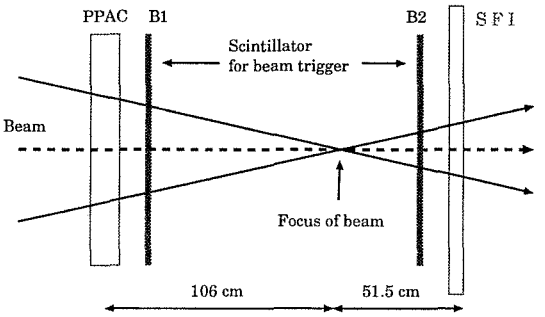

Figure 6: Layout of detectors in ^{58}Ni beam measurement. PPAC is the position sensitive Parallel Plate Avalanche Counter [10]. B1 and B2 are plastic scintillation beam counters.

The position sensitive Parallel Plate Avalanche Counter (PPAC) was placed in front of the focus plane in order to obtain the beam profiles[10]. The incident beam was defined by two plastic scintillation beam counters, B1 and B2. The effective area was smaller than that of SFI. The SFI was installed behined the B2 counter. The beam trigger was defined by B1*B2. In order to extract the cross-talk information, the MAPMT anode signals of *passing-through* beams were send to Analog-to-Digital Converter (ADC).

Figure 7a shows the examples of pulse height distribution obtained with one anode, where the highest pulse are selected in all anodes for one beam event. Then, Figure 7b shows the pulse height distribution of neighboring anode at the same event.

We found, that 40 - 50% the scintillated photons from the edge of the fiber were collected by neighbors. If we can avoid this cross-talk, the detection efficiency for the RLGS map would increase. Therefore to improve the detection efficiency, we started to develop a new detector attached to another type of MAPMT that has four times larger anode area than the above mentioned one .

Furthermore, we have measured the image of ^{58}Ni beam to investigate the system's applicability to nuclear

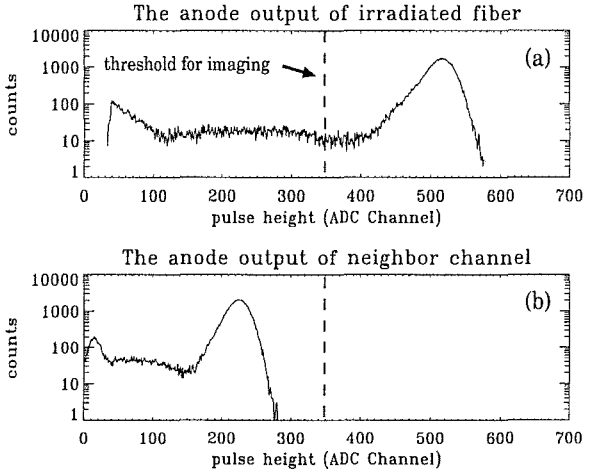

Figure 7: Pulse height spectra of ^{58}Ni beam: (a) Spectrum of anode output of irradiated fiber. (b) Spectrum of anode output for neighboring fiber. The threshold should be set to the level shown by the arrow to reach position sensitivity.

physics experiments. In order to decode the incident position, we should avoid the multiple trigger with the neighboring channels. Thus the discriminator thresholds were set to just below the main pulse height of the beam, shown by the arrow in Figure 7.

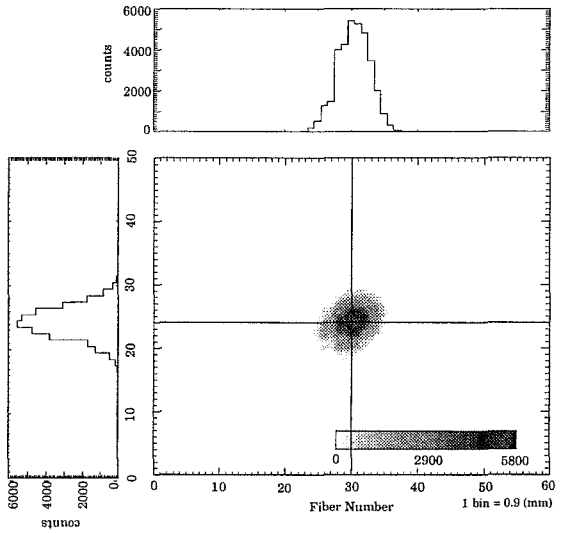

Figure 8: The measured image of ^{58}Ni beam at 90 AMeV

Figure 8 shows the measured image of the ^{58}Ni beam. The SFI detector was installed at the distance of 51.5 cm from the focus of the beam. The resulted beam size is 5.4 mm (FWHM) for X-axis and 5.3 mm (FWHM) for Y-axis. The PPAC[10] detector, installed at the distance of 106 cm, also detected the beam size 10 mm (FWHM). Taking into the account the distance from focus, these results are consistent.

The detection efficiency of this detector was 70% compared to the beam trigger. The main source of the reduced detection efficiency is the 74% effective area of SFI to vertical incident beam.

V. Conclusions

We had developed a Scintillating Fiber Imager (SFI) applicable to measurement of Restriction Landmark Genomic Scanning (RLGS) map. The SFI consists of two orthogonal fiber-layers that includes two sets of 256 fibers. The 256 fibers could be read out by two sets of 16 channels Multi-Anode PhotoMultiplier Tube (MAPMT) using a special encoding method, hence we succeeded in reducing the number of readout channels of the 1024 fibers to 128 channels. The SFI has a large effective area of 43 x 43 cm^2 that can cover a gel sheet. We carried out test measurements for RLGS map labeled with ^{32}P (β-ray emitter). We succeeded in reducing the time required for measurement to 50 hours and to see the image in real-time. However, the measuring time was longer than we expected because of photon cross-talk between fibers and photo-cathode of MAPMT. We estimated the cross-talk ratio to 40 - 50% by a measurement of heavy ion (^{58}Ni beam at 90 A MeV) beam.

Furthermore, we tested the performance of our system as a position sensitive detector for heavy ions. The detection efficiency of SFI is 70% of the beam trigger and its position resolution is comparable to a position sensitive Parallel Plate Avalanche Counter (PPAC) detector. We have shown the SFI is applicable to not only β-ray but also heavy ion detection.

VI. Acknowledgments

This work was supported by the project of Core Research for Evolutional Science and Technology (CREST) of Japan Science and Technology Corporation (JST). We are grateful to the members of the Genome Science Laboratory of RIKEN who provided us the sample of RLGS maps. We thank the members of the RIKEN accelerator facilities who provided us the beam. We thank Dr. K. Kuroda for valuable discussions. We thank Dr. N. Iwasa for providing us the CAMAC data taking program.

VII. References

[1] Y. Hayashizaki et al, "Restriction landmark genomic scanning method and its various application," *Electrophoresis, vol. 14, 1993* pp. 251-258.

[2] Y. Hayashizaki et al, "A Genetic Linkage Map of the mouse using restriction landmark genomic scanning," *Genetics, 138, 1994* pp. 1207-1238.

[3] J. Cub et al, "A large-area scintillating fiber detector for relativistic heavy ions," *Nucl. Inst. and Meth., A 402, 1998* pp. 67-74.

[4] V. Agoritas et al, "Read-out of scintillating fibers using a weak cross-talk position-sensitive photomultiplier," *Nucl. Inst. and Meth., A 406, 1998* pp. 393-402.

[5] M. Leblanc et al, "SOFI: A scintillating optical fiber

imager," *Nucl. Inst. and Meth., A 273, 1988* pp. 583-587.
[6] M. Bendai et al, "Scintillating optical fiber detectors for DNA sequencing," *Nucl. Inst. and Meth., A 310, 1991* pp. 373-378.
[7] Bicron Catalogue on Scintillating Optical Fiber
[8] Hamamatsu Catalogue on Photomultiplier Tubes and Assemblies (For Scintillation Counting & High Energy Physics)
[9] Hamamatsu Photonics technical data sheet on Multianode Photomultiplier Tube (R5900 series)
[10] H. Kumagai et al, "PPAC for Beam Profile Monitor at the RIPS" *RIKEN Accel. Prog. Rep. 28, 1995* pp. 127.